Sorption-Induced Release of Antimicrobial Isopropanol in EVOH Copolymers as Determined by ATR-FTIR Spectroscopy

D. Cava,[1] C. Sammon,[2] J. M. Lagaron[1]

[1]*Institute of Agrochemistry and Food Technology, CSIC, 46100 Burjassot, Spain*
[2]*Materials and Engineering Research Institute, Sheffield Hallam University, Sheffield, S1 1WB, United Kingdom*

ABSTRACT: This paper deals with the evaluation of the sorption-induced release of an antimicrobial component, i.e., isopropanol, from two ethylene-vinyl alcohol (EVOH) copolymers as measured by ATR-FTIR spectroscopy. Three different swelling agents were considered namely, water, methanol, and ethanol, whose kinetics of diffusion were also evaluated during sorption. From the transport behavior of the latter components, it was found that a pseudo-Fickian diffusion process appeared to take place in all systems. The corresponding simultaneous polymer plasticization was easily followed by evaluation of the sorption-induced thickness expansion and swelling rate. The data indicated that the swelling process appeared to lag the sorption of the penetrant during the first instances of the uptake most probably due to the existence of a Langmuir (antiplasticization) regime previously reported for these polymers. The crossed-diffusion of entrapped antimicrobial isopropanol was related to a typical swelling-induced release process, which was found to be strongly dependent on the nature of the penetrant and on the composition of the polymer matrix. The results demonstrated both the usefulness of the ATR-FTIR technique to uniquely characterize the complex phenomena that take place during sorption-induced release and the suitability of EVOH copolymers for controlled release in antimicrobial applications. © 2006 Wiley Periodicals, Inc. J Appl Polym Sci 103: 3431–3437, 2007

Key words: diffusion; controlled release; infrared spectroscopy; EVOH copolymers

INTRODUCTION

The use of swellable materials for the release of active and bioactive compounds has been widely known for many years. These materials can have a synthetic nature or be isolated from biomass resources. In these systems, the release of desired components occurs mainly by counter-transport of the solvent "in" and diffusion "out" of the component through the swollen polymer. In general, these materials are in a "glassy" state at room temperature and as the solvent penetrates, it causes stresses, which are accommodated by an increase in the radius of gyration and end-to-end distances, which lead to macroscopic swelling and T_g drops to below room temperature. Thus, the solvent molecules move into the glassy polymer matrix with a well-defined front at a particular rate and, simultaneously, the thickness of the rubbery or swollen region increases with time in the opposite direction. This usually drives the kinetics of transport into typical "Case II" diffusion modes. Case II diffusion is defined when linear behavior is observed in the normalized uptake versus t (time) curve. This behavior is observed in a number of these swellable systems and is associated with large uptakes and plasticization of the structure by the penetrants.[1,2]

Ethylene-vinyl alcohol (EVOH) copolymers have become, because of their low permeability to gases and organic vapors, one of the most widely used high barrier family of materials.[3] EVOH properties are known to be strongly related to ethylene content, as a result, commercial grades vary from high to low contents depending on the end application. Thus, copolymers with higher ethylene contents have higher oxygen permeability, but are less affected by water sorption and *vice versa*. Previous studies on this polymer showed that:

1. Sorption of water and methanol in EVOH32 are relatively high; for water ~9% W/W_{dry} and for methanol ~12% W/W_{dry}.
2. Uptake rates do not show Fickian behavior.[4]

However, the extensive plasticization of these systems by sorption of polar solvents such as alcohols

and water and its dependency on factors such as composition and crystallinity have previously been exploited for sorption-induced controlled release of active and bioactive substances of interest. Moreover, the safety, biocompatibility, and biodegradability of these polymers, reflected by its use for instance as hemodialysis membranes, allow their use in biomedical and drug release applications.[1] Thus, previous gravimetric studies on the use of these materials for controlled-release indicated that the sorption of alcohols is lower with increasing the molar mass of the penetrants, e.g., depending on composition the uptake of methanol is, for instance, reported to be between 13 and 16%, between 2 and 4% for ethanol, between 2.1 and 2.4% for propanol, and between 2.6 and 3% for butanol. This study further described the release of theophylline from porous systems of these copolymers and found that porosity and the degree of crystallinity were affecting the release process.[5] Another work detailed the release of sodium chloride and of a high-molecular-weight dye (malachite green) as a result of water sorption for some of these copolymers saturated in the releasing components. From the results it is evident that sodium chloride essentially followed the sorption and subsequent plasticization of the polymer, whereas the dye had Fickian desorption patterns and its diffusion ''out'' lagged with respect to the rapid swelling of the polymer.[6] To evaluate these complex cross-diffusion events, different methodologies have been employed, which are often not direct and do not allow the simultaneous or *in situ* study of the overall processes involved.

In this context vibrational spectroscopy, generally ATR-FTIR spectroscopy, has proven to be a unique tool to fully characterize polymer-penetrant transport properties and its associated phenomena, as it is possible to obtain sorption and diffusion parameters and information about polymer-penetrant interactions from the same experiment.[7–9] It is also relatively straight forward to simultaneously obtain information related to the polymer membrane such as changes in morphology and swelling. The potential of the technique has already been proven in previous studies, which focused on the determination of the transport properties of aroma and food components and active packaging additives in polymeric films using FTIR methodologies.[10–12] This technique is particularly useful for measuring transport properties in the transmission mode through very thin films, such as those usually considered in multilayer food packaging applications, and to simultaneously characterize the transport of multiple permeants as is also the case in most real situations.[12,13]

One of the challenges that needs be addressed when using ATR-FTIR spectroscopy to follow the dissolution kinetics of an active membrane in a matrix is to achieve a good interfacial contact between

the free standing sample and the ATR crystal. There have been several approaches to this problem and the best solution will ultimately be determined by the nature of the membrane. Wartewig and coworkers have modified the geometry of such measurements to incorporate an acceptor layer between the donor (i.e., drug formulation) and membrane to be studied.[14–17] A number of examples of this approach are given in a review by Wartewig[18] and the reader is advised to examine this article and the references therein for more detail. Recently Kazarian et al.[19,20] have used ATR-FTIR imaging to study the hydration and dissolution kinetics of a number of HPMC-based binary pharmaceutical formulations. One of the major innovations of this work was the design (and subsequent validation) of a compaction cell to study these systems; maintaining a good optical contact between the sample and the ATR crystal while allowing water (or some other dissolution medium) unrestricted access to the tablet surface.[19,20] This method is really applicable only to compactable materials. Nevertheless, polymer dissolution followed by solvent evaporation, i.e., solution casting, is often a very simple route to achieve adequate contact, which can be scaled up via industrial processes such as solvent evaporation coating or lamination technologies.

This study reports, for the first time, the use of ATR-FTIR spectroscopy to follow the kinetics of sorption of water, methanol, and ethanol and to study the simultaneous sorption-induced controlled-release of isopropanol as a function of EVOH polymer composition. It is also proposed to simultaneously characterize the polymer sorption-induced rate and degree of swelling. The interest and synergies of isopropanol arise from the fact that, on the one hand, it dissolves the polymer and, therefore, it can be entrapped in the material by a casting process; and, on the other hand, this alcohol is an antimicrobial component, which has been found to be slightly more bactericidal than ethanol and is known to exhibit great activity against both *Escherichia coli* and *Staphylococcus aureus*.[21] The use of EVOH as an antimicrobial carrier with swelling-induced controlled release capacity could be of great interest in many applications within fields such as biomedical, health care, and active packaging.

EXPERIMENTAL

Materials

Two different commercial ethylene-vinyl alcohol copolymer grades (Soarnol) supplied by The Nippon Synthetic Chemical Industry (NIPPON GOSHEI) (Japan) were analyzed: EVOH29 and EVOH44, where the number indicates the mole percentage of ethylene

in the copolymer composition. Distilled water and highly purified research grades of isopropanol (99.99), ethanol (>99.9) and methanol (>99.5%) purchased from Acros Organics (Gent, Belgium) were the penetrants used. These two materials are extreme in composition and properties among the most commonly used EVOH commercial grades.

Methods

Preparation of EVOH films

These materials were dissolved in mixtures of isopropanol/water (70/30 v/v) at 70°C, subsequently cast onto the ATR crystal (to ensure intimate contact between the sample and the ATR crystal) and dried at 70°C until no trace of the water band at 1654 cm^{-1} was observed and the intensity of the isopropanol band at 951 cm^{-1} remained constant in the ATR-FTIR spectrum. Different drying conditions were applied and it was found that direct drying with no gas purging at relatively mild temperatures over a hot surface, i.e., the ATR hot plate, appeared to yield best results regarding water release and isopropanol entrapment. After preconditioning, an ATR flow cell was mounted over the film, then the temperature was lowered to 30°C and the sample was put in contact with an infinite reservoir of the permeants as described in previous papers by the authors.[7,9,13]

ATR-FTIR measurements

ATR-FTIR spectra were collected using a temperature controlled Golden Gate^{TM} single reflection diamond ATR accessory (SpectraTech) coupled to a Thermo Nicolet Nexus FTIR spectrometer. Polymer formulations were solution cast to ensure direct contact with the ATR crystal as described previously. Data were collected by averaging 10 scans at 4 cm^{-1} resolution at predefined time intervals. Both the blank ATR crystal and the "dry" polymer film at the same temperature under the same conditions were used as reference backgrounds. All data were manipulated using Omnic 6.1 software supplied by ThermoNicolet and the ATR-FTIR experiments were carried out, at least, in duplicate. From the experiments mean and standard error values were reported.

Modeling diffusion data

Data fitting to a suitable model is required to derive a quantitative measure of diffusion kinetics from experimental curves obtained using ATR-FTIR spectroscopy. To obtain D values from these sorption curves, the experimental curves must be fitted to the appropriated solution of Fick's second law of diffusion for the case of a plane sheet [eq. (1)] modified to suit an

ATR experiment [eq. (2)] as proposed by Fieldson et al.[8]:

$$\frac{M_t}{M_\infty} = 1 - \sum_{n=0}^{\infty} \frac{8}{(2n+1)^2\pi^2} \exp\left[\frac{-D(2n+1)^2\pi^2 t}{4L^2}\right] \quad (1)$$

$$\frac{A_t}{A_\infty} = 1 - \frac{8\gamma}{\pi\left[1 - \exp(-2\gamma L)\right]}$$

$$\times \sum_{n=0}^{\infty}\left[\frac{\exp\frac{-D(2n+1)^2\pi^2 t}{4L^2}\left[\frac{(2n+1)\pi}{2L}\exp(-2\gamma L) + (-1)^n(2\gamma)\right]}{(2n+1)\left(4\gamma^2 + \frac{(2n+1)\pi}{2L}\right)}\right]$$

$$(2)$$

where A_t and A_∞ are the spectral absorptions at a time t and equilibrium, respectively, and d_p is the penetration depth.

$\gamma = 1/d_p$, D is the diffusion coefficient, and L is the film thickness.

However, in an analogous manner to that described in previous works by these and other authors, a simplified approach was used to determine D values, which is based on an observed initial "lag" time (normalized to path length L), during which little sorption occurs within the evanescent field, followed by a pseudo-Fickian ($\sqrt{t}$ power law) behavior predicted from eq. (1) at short times:

$$\frac{M_t}{M_\infty} = \frac{2}{L}\left(\frac{D}{\pi}\right)^n t^n \quad (3)$$

where $n = 0.5$.

RESULTS AND DISCUSSION

Figure 1 shows the ATR-FTIR spectra of EVOH29 and EVOH44 and of pure water, methanol, ethanol, and
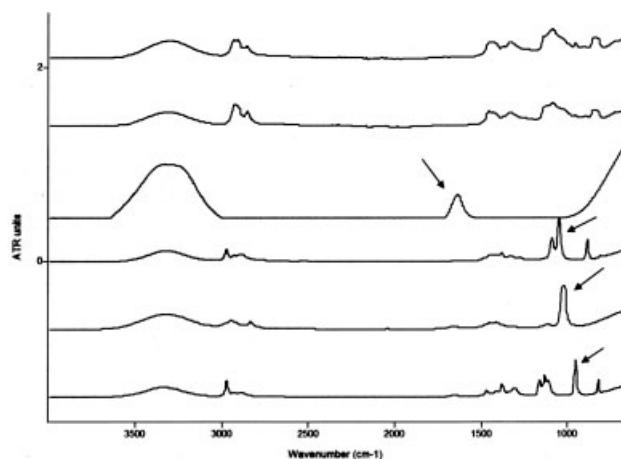

Figure 1 ATR-FTIR spectra of from top to bottom, EVOH29, EVOH44, water, ethanol, methanol, and isopropanol. Arrows indicate the bands used for the calculations.
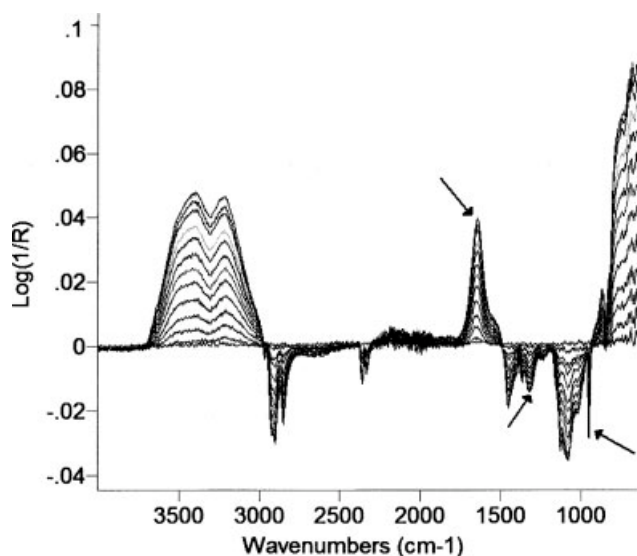
Figure 2 ATR-FTIR spectra after subtraction of the polymer during sorption of water in EVOH44. The arrows indicate from left to right the bands used for water, thickness variations, and isopropanol calculations.

isopropanol. From Figure 1 it can be observed that each component has got discrete diagnostic bands, the intensity change of which with time can be used to determine diffusion coefficients. The best candidate band for the analysis of the water sorption process is the 1635 cm^{-1} OH bending vibration. This band does no overlap with the polymer signal and does not shift over the sorption process.[22] Frequency shifts are undesirable when determining diffusion coefficients using infrared spectroscopy as significant changes in absorption coefficients may occur at the same time, which cannot be distinguished from changes in concentration during the sorption process. For methanol and ethanol the most appropriate bands are 1019 and 1046 cm^{-1} assigned to the alcohol $\nu(CO)$. These bands are very intense in the spectrum but as they overlap to some extent with the polymer signal, to estimate the

penetrants band area the signal was subtracted from the corresponding polymer signal recorded at each time instance during the course of the sorption. The polymer signal at each time interval is different due to thickness variations across the experiment and hence the need for this particular correction.

Figure 2 shows, as an example, the subtraction spectra of the penetrant water after subtraction of the neat EVOH44 polymer. From this figure the existence of positive and negative bands becomes evident. Positive bands mean sorption of the penetrant, while the existence of negative bands indicates loses of trapped components and polymer swelling as a result of the penetrant sorption. The ATR-FTIR spectroscopy is unique in its ability to simultaneously determine both of the cited effects. It is worth noting the presence of a negative contribution at 951 cm^{-1} assigned to isopropanol trapped in the polymer solid structure. Polymer dissolution and casting is thus an effective way to enclose substances of interest such as active and bioactive components in polymer and biopolymer matrices for controlled release or migration of active and bioactive substances. The presence of trapped isopropanol in the structure of the polymer is confirmed by the presence of the isopropanol CH bending band at 951 cm^{-1} in EVOH29 as well as in EVOH44. This band is seen to decrease, albeit to a different extent, and disappears as the different penetrant components sorb "into" and plasticize the polymer molecular structure (see Figs. 3 and 4). This technique shows, therefore, a great potential for the study of these polymers in applications where controlled release of trapped substances is required, triggered by for instance environmental humidity or by sorption of certain selected swelling components.

Figures 3 and 4 show the sorption curves of water, methanol and ethanol into EVOH29 and EVOH44 and the corresponding associated desorption of isopropanol. The inset in Figure 3 magnifies the initial sorption of water and methanol for a better discrimination
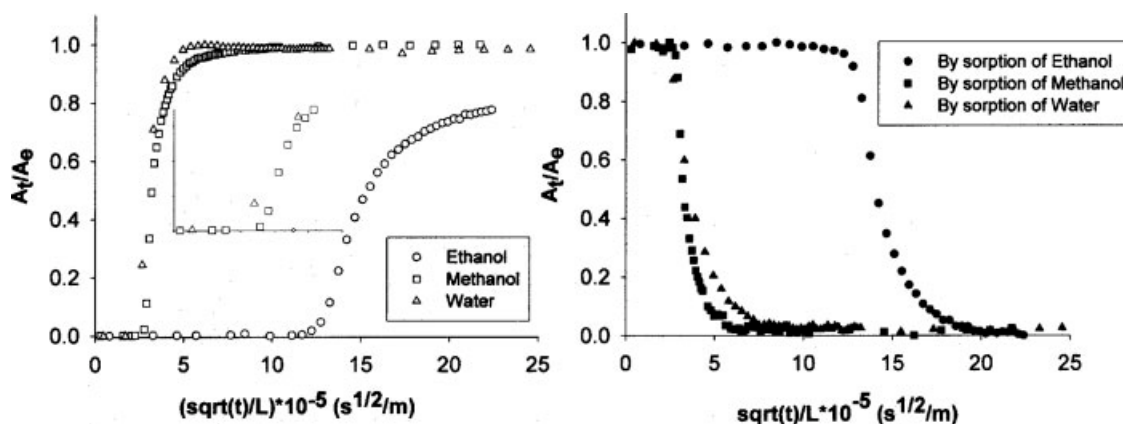

Figure 3 Sorption (right) of water, methanol, and ethanol and release (left) of isopropanol during sorption of these in EVOH29. The right graph inset details the initial steps during sorption for water and methanol for comparison purposes.
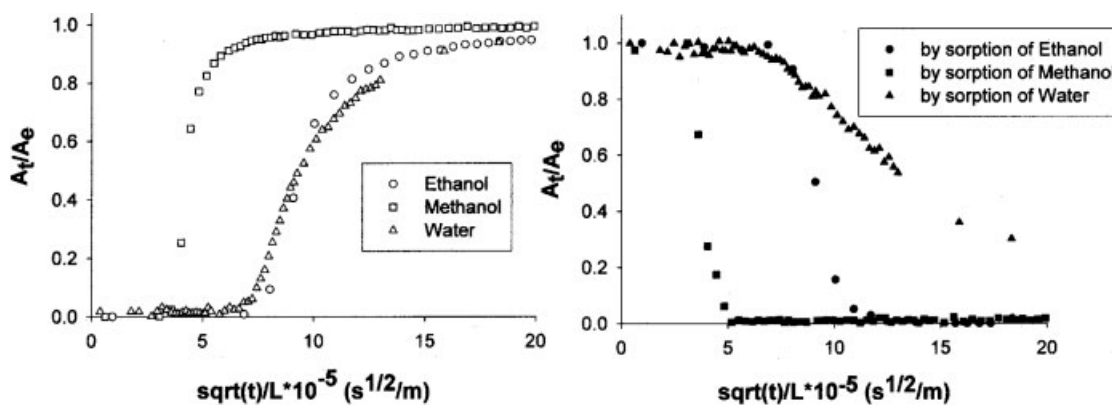
Figure 4 Sorption (right) of water, methanol, and ethanol and release (left) of isopropanol during sorption of these in EVOH44.

between the two components. The figures indicate that there is an initial "induction time" period before penetrant sorption, which is related to the time span needed for the permeant to reach the evanescent field. Usually this induction time is larger for penetrants with slower kinetics. The observation of the normalized uptake versus $t^{0.5}$ indicates that a reasonable straight line can be drawn up during the beginning of the sorption process. This later departs from linearity and arrests near equilibrium. The latter behavior suggests that an anomalous Pseudo-Fickian diffusion mode is present for all penetrants. Table I gathers the estimated diffusion coefficients measured for the various systems during the first stages of the sorption event and also of isopropanol during the simultaneous desorption in EVOH29 and EVOH44. From Figures 3 and 4 and Table I it is clear that: (i) diffusion rates are faster in EVOH29 for methanol and water and slower for ethanol and (ii) in EVOH44 diffusion rates are faster for methanol and slower for ethanol and water. This appears reasonable and in accordance with previous studies, which indicated that for the case of EVOH32, more similar to the EVOH29 grade studied here, the uptake and sorption rate were found to be higher for methanol and water and lower for ethanol, which is a bigger molecule and with less hydrophilic character. In the case of EVOH44, as the polymer composition becomes less polar, with an enlarged free volume when compared to EVOH29, methanol still diffuses faster than ethanol and water, which is probably influenced by molecular size and repulsive hydrophobic forces. Another interesting observation is that the diffusion of methanol and water are faster in EVOH29 than in EVOH44 but diffusion of ethanol goes faster in EVOH44 due to the larger size and less polar character of the later molecule. Summarizing, diffusion is the fastest for methanol in EVOH29 and is the slowest for water in EVOH44; but the largest difference in diffusion rate for the penetrants is for water, which has an approximately 16-fold difference in diffusion coefficient depending on whether it penetrates EVOH29 or 44.

Nevertheless, the most interesting result of this study comes from the observation of the simultaneous release of isopropanol during sorption of the three components and how the nature of the diffusing species affects its release rate. The first general observation concerning isopropanol release, arising from Figures 3 and 4, is that the release of this component is faster in EVOH29 when the diffusing species are methanol or water. Thus, Figure 3 indicates that the induction time for the release of isopropanol from EVOH29 formulations is clearly smaller during the sorption of methanol and water than during the sorption of ethanol. This is of course in agreement with the faster diffusion and subsequent sorption-induced plasticization of EVOH by the incoming water and methanol. The proposed release mechanism for this component is based on several contributions: the severe plasticization (enlarged free volume) of the polymer produced by penetrant sorption, the cross-diffusion "out" of the isopropanol, and its dissolution in the penetrants, and the affinity of the penetrants for

TABLE I
Sorption Diffusion Coefficients and Swelling Rate Factors for Ethanol, Methanol, and Water and Release Diffusion Coefficient for Isopropanol in EVOH29 and EVOH44

	Ethanol	Methanol	Water
EVOH29			
D^a	28.10 ± 4.63	1410 ± 24.80	643.40 ± 100
$D_{Isopropanol}$	76.30 ± 18.52	1210 ± 86.50	151 ± 19.10
Swelling rate^b	0.03 ± 0.01	1.67 ± 0.30	0.64 ± 0.12
EVOH44			
D	47.63 ± 21.10	521 ± 183	40 ± 2.68
$D_{Isopropanol}$	109 ± 17.40	440 ± 16.10	3.79 ± 1.22
Swelling rate	0.16 ± 0.04	3.46 ± 0.80	0.05 ± 0.01

^{a} $D \times 10^{13}$ (all values expressed in m^2/s).
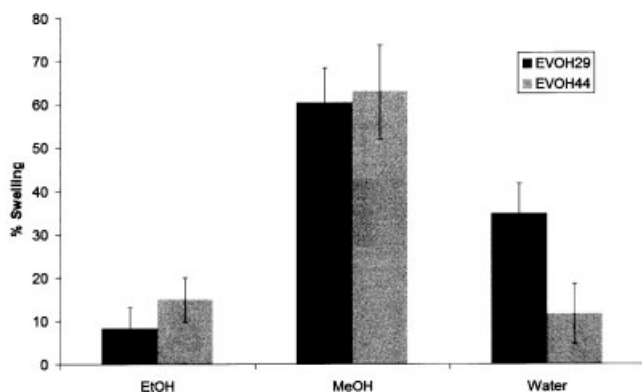^{b} Swelling rate factor (% sw/s).

Figure 5 Percentage swelling factor for water, methanol, and ethanol in EVOH29 and 44.

the polymer that results in replacement of isopropanol at the polymer hydrophilic sites.

Comparison of the relative rates of isopropanol release versus water/methanol/ethanol diffusion coefficients, which are summarized in Table I, indicates that the diffusion of isopropanol from EVOH29 is faster during sorption of ethanol than during the diffusion-in rate of ethanol, it is lower for water and is similar for methanol. The fact that ethanol and water diffusion coefficients are quite different than the corresponding isopropanol dissolution rate indicates that the release mechanism is not simply one of displacement, although for methanol this may seem like it. Nevertheless, methanol, and to a certain degree ethanol, would appear to facilitate the release of isopropanol more readily from the polymer-free volume than water. Another very interesting observation, which is only made possible in ATR experiments, is that even when the induction time (time for the permeant to reach the evanescent field or the measurable sample area in contact with the ATR crystal) is quite similar for both methanol and water sorption and the associated desorption of isopropanol (see Fig. 3), the actual estimated diffusion coefficients (relating to the kinetics of desorption from the evanescent field sample area) (see Table I), are somewhat differing; they are slower for water. Some inconsistencies between induction times and estimated diffusion coefficients are probably related to lack of Fickian behavior in the systems.

For the sample EVOH44, shown in Table I and Figure 4, it appears that the dissolution of isopropanol is slower than for samples of EVOH29, except during the sorption of ethanol. However, in accordance with the EVOH29 case, the release of isopropanol from EVOH44 is observed to be faster during the sorption of methanol and ethanol than during sorption of water. In this case, analogous to the EVOH29 system, the rates of sorption of these components appear to match only the dissolution rate of isopropanol when the ''sink'' media is methanol. From a controlled

release view point it appears that release rates could be accelerated by the incorporation of methanol in copolymers with low ethylene content and that to achieve slower release rates, water should be used as the release trigger media in combination with copolymers comprising high ethylene molar contents. A further study will deal with the effect of relative humidity on the biocide release, and it is expected that lower water activities in low ethylene content copolymers will lead to lower values of release rate for this and other biocide components.

Another curious observation in Table I and Figure 4 is that while the diffusion of ethanol and water is similar for EVOH44, the associated release rate of isopropanol is faster for the case of the former component. The reason for that may be related to the fact that the sorption of ethanol leads to a higher swelling rate of the polymer than sorption of water, as indicated by Table I. This higher swelling rate may facilitate the desorption of the antimicrobial molecule.

ATR-FTIR spectroscopy is also capable of determining thickness changes during the penetration of plasticizing components, which result in swelling of the polymer topology. The sorption of all of the components in the systems considered in this work leads to plasticization of the polymer matrix to a higher or lower extent. Figure 5 shows the swelling factor as a percentage of sample thickness expansion for all penetrants and materials, estimated from changes in the area of the polymer band centered at 1333 cm^{-1} (pointed with an arrow in Fig. 2). Figure 6 shows, as an example, the plot of the relative uptake of methanol and ethanol in EVOH29 versus the corresponding relative swelling. From the latter Figure, it is seen that there appears to be a linear correlation between the two events, but only after 35% of the sorption process has taken place. Below 35%, it seems that the swelling
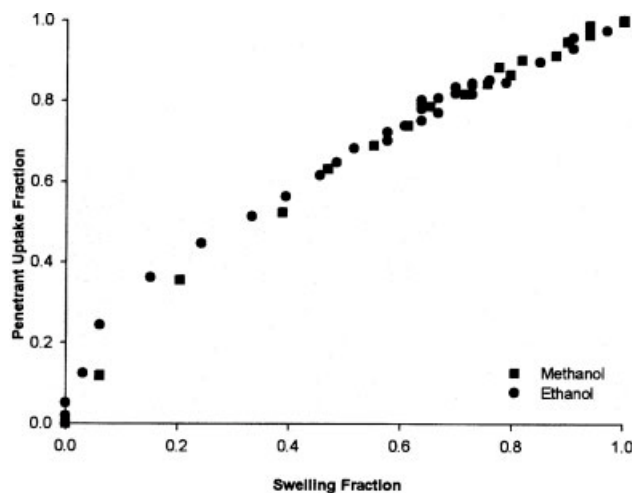

Figure 6 Normalized swelling versus normalize sorption for methanol and ethanol in EVOH29.
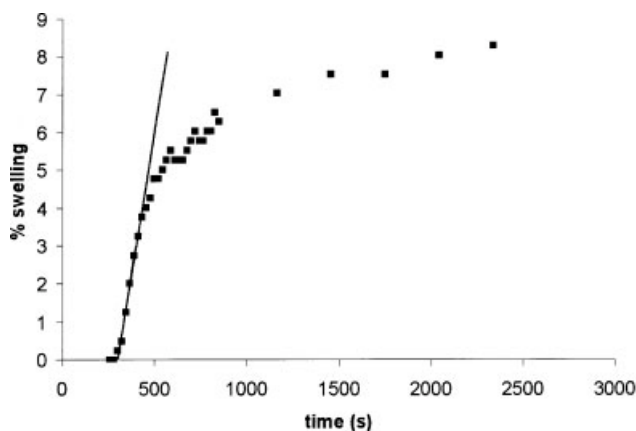
Figure 7 Swelling percentage versus time for ethanol in EVOH29.

process does actually lag the sorption of penetrants. In fact, it appears that the higher the uptake, the lower the lag between the two events, as would be expected from the fact that higher sorption entails higher plasticization and hence faster swelling. The reason for the existence of a lag in swelling with regard to penetrant sorption can be explained on the basis of previous observations made during water sorption and oxygen permeability as a function of water activity for these polymers.[7,23] Previous studies indicated that for these materials, there is a Langmuir regime below ~35% RH[31] during which water molecules tend to fill in the available "free volume" and block the passage of oxygen, therefore leading to even lower permeability than under dry conditions, i.e., so called antiplasticization effect. Under these circumstances, it would be expected that sorption-induced swelling would begin to follow the uptake only after this initial Langmuir regime is superseded. Similar results were found for the other penetrants and for EVOH44 and, therefore, a similar behavior can be drawn for the other permeants and copolymer (results not shown).

Turning back to Figure 5, it can be seen that the highest sorption-induced swelling (around 60%) occurs for methanol in EVOH44 and 29. In good agreement with changes in the diffusion coefficient, swelling is higher in EVOH29 for methanol and water and is lower for ethanol, whereas for EVOH44 swelling is higher for methanol and ethanol and is lower for water. Thus, swelling is higher for methanol in EVOH29 and lower for water in EVOH44 and so is the diffusion release rate of isopropanol in these systems. The larger differences in swelling for water in the two polymers are reflected by the more of one order of magnitude difference (16 fold) between the measured diffusion coefficients. However, although methanol goes only about three times faster in EVOH29 compared to EVOH44, it seems to swell the two polymers to a similar extent or even more for the case of EVOH44. The reason for this behavior rests on

the fact that it is the uptake (solubility coefficient), and not the diffusion coefficient, the responsible factor for swelling; the diffusion coefficient defining only the rate of swelling. As a consequence of all of the above, it is therefore conclusive that the release of isopropanol is a direct consequence of sorption-induced swelling in the polymers but also of replacement from the polymer hydrophilic sites by the penetrants, which generate stronger hydrogen bonding interactions.

Finally, Table I also gathers the estimated swelling rate factors for all permeants in EVOH29 and EVOH44. The swelling rate factor is defined as the initial linear slope of the thickness expansion versus t (time) curves (see Fig. 7 for an example). From these results it appears that higher initial swelling rates occur for methanol in EVOH44 and then in EVOH29 in agreement with the higher final swelling values in Figure 6. Water swells faster than ethanol in EVOH29 and slower in EVOH44, which observation is also in agreement with data plotted in Figure 6.

References

1. Ranga Rao, K.V.; Padmalatha Devi, K. Int J Pharm 1988, 48, 1.
2. Colombo, P. Adv Drug Delivery Rev 1993, 11, 37.
3. Lagaron, J. M.; Catala, R.; Gavara, R. Mater Sci Technol 2004, 20, 1.
4. Lagaron, J. M.; Powell, A. K.; Bonner, J. G. Polym Test 2001, 20, 569.
5. Segot-Chicq, S.; Peppas, N. A. J Controlled Release 1996, 3, 193.
6. Hopfenberg, H. B.; Apicella, A.; Saleeby, D. E. J Membr Sci 1981, 8, 273.
7. Sammon, C.; Yarwood, J.; Everall, N. Polymer 2000, 41, 2521.
8. Fieldson, G. T.; Barbari, A. T. Polymer 1993, 34, 1146.
9. Döppers, L. M.; Breen, C.; Sammon, C. Vib Spectrosc 2004, 35, 27.
10. Lagaron, J. M.; Giménez, E.; Gavara, R.; Catala, R. Macromol Chem Phys 2003, 204, 704.
11. Lagaron, J. M.; Cava, D.; Giménez, E.; Hernandez-Muñoz, P.; Catala, R.; Gavara, R. Macromol Symp 2004, 205, 225.
12. Cava, D.; Catala, R.; Gavara, R.; Lagaron, J. M. Polym Test 2005, 24, 483.
13. Döppers, L. M.; Sammon, C.; Breen, C.; Yarwood, J. Polymer, to appear.
14. Hartmann, M.; Hanh, B. D.; Podhaisky, H.; Wensch, J.; Bodzenta, J.; Wartewig, S.; Neubert, R. H. H. Analyst 2004, 129, 902.
15. Hanh, B. D.; Neubert, R.; Wartewig, S. Int J Pharm 2000, 204, 145.
16. Hanh, B. D.; Neubert, R.; Wartewig, S. Int J Pharm 2000, 204, 151.
17. Hahn, B. D.; Neubert, R.; Wartewig, S. Christ, A.; Hentzsch, C. J Pharm Sci 2000, 89, 1106.
18. Wartewig, S.; Neubert, R. H. H. Adv Drug Delivery Rev 2005, 57, 1144.
19. Chan, K. L. A.; Kazarian, S. G. Vib Spectrosc 2004, 35, 45.
20. Kazarian, S. G.; Chan, K. L. A. Macromolecules 2003, 36, 9866.
21. Paulson, D. S.; Fendler, E. J.; Dolan, M. J.; Williams, P. A. Am J Infect Control 1999, 27, 332.
22. Sammon, C.; Bajwa, G.; Timmins, P.; Melia, C. Polymer 2006, 47, 577.
23. Cava, D.; Cabedo, L.; Gimenez, E.; Gavara, R.; Lagaron, J. M. Polym Test 2006, 25, 254.